Spectrochimica Acta Part A: Molecular and Biomolecular Spectroscopy 238 (2020) 118431

Contents lists available at ScienceDirect

Spectrochimica Acta Part A: Molecular and Biomolecular Spectroscopy

journal homepage: www.elsevier.com/locate/saa

Thiazolidine based fluorescent chemosensors for aluminum ions and their applications in biological imaging

Duygu Aydin [b,*], Emel Karakilic [a], Serdar Karakurt [c], Arif Baran [a,*]

[a] Sakarya University, Department of Chemistry, Sakarya 54187, Turkey
[b] Karamanoglu Mehmetbey University, Department of Chemistry, Karaman 70100, Turkey
[c] Selcuk University, Department of Biochemistry, Konya 42031, Turkey

ARTICLE INFO

Article history:
Received 15 March 2020
Received in revised form 27 April 2020
Accepted 27 April 2020
Available online 03 May 2020

Keywords:
Thiazolidine
Fluorescence sensor
Aluminum

ABSTRACT

Utilization of fluorescent techniques in detection of various metal ions actively pursued allow ultrasensitive and selective detections of metal ions and prevent the adverse effect of cations such as aluminum (III) ions. In this study, two novel fluorescent chemosensors containing thiazole derivatives, ((E)-2-(4-hydroxy-3-(((2-hydroxyphenyl)imino)methyl)phenyl)-3-phenyl thiazolidin-4-one) **AM1** and (2,3-bis(4-hydroxy-3-((E)-((2-hydroxyphenyl)imino) methyl) phenyl) thiazolidin-4-one) **AM2**, have been fabricated. The probes **AM1** and **AM2** were prepared using the condensation reaction between 2-hydroxy-5-(4-oxo-3-phenyl thiazolidin-2-yl) benzaldehyde and 2-aminophenol for the probe **AM1** and 5,5′-(4-oxothiazolidine-2,3-diyl)bis(2-hydroxy benzaldehyde) and 2-aminophenol for the probe **AM2**. Afterwards, they were analyzed by various types of NMR and FT-IR spectroscopy, ESI-MS spectra, and elemental anayzer. As a second step, each fabricated chemosensor was able to use turn on fluorescence sensing for detecting of Al^{3+} ions in ACN/H_2O (v/v = 50/50, 10.0 μM, pH = 7.0) solution. Clear complexes formed between the probe **AM1** and Al^{3+} ions and also the probe **AM2** and Al^{3+} ions was determined by not only ^1H NMR titration study but also calculated by using the Job's plot. The limit of detection (LOD) value was found to be 0.11 μM (**AM1**) and 4.4 μM (**AM2**) for Al^{3+} ions. Likewise, cell imaging and in vitro cytotoxicity experiments of Al^{3+} ions in Human epithelium Lovo cells exhibited that prepared chemosensors had low cytotoxicity and blue fluorescence when they treated with of Al^{3+} ions in the cellular system.

1. Introduction

Al^{3+} ion is the maximum abundant d-block metal ions in the earth behind iron and zinc and compounds of Al^{3+} have a vital role in water purification, food additives, clinical drugs, the production of light alloys, the paper industry, clinical therapy and so on. Aluminum (III) ions have been widely utilized in daily life for example, in food, aluminum-based pharmaceuticals, drinking water sources, environmental and biological sources and kitchen utensils [1–3]. However, high concentration of aluminum is harmful to the environment systems and human health since its toxicity may induce wide range of diseases, for example dialysis encephalopathy, osteomalacia, Parkinson's and Alzheimer's disease breast cancer and etc. [4–8]. The World Health Organization (WHO) has reported that the maximum admissible level of weekly human intake of Al^{3+} is about 3 mg/day of the body weight. Therefore, monitoring trace amounts of aluminum ions in environmental monitoring and biological assays are highly demanded [[9–12]].

Numerous analytical methods, atomic absorption/emission spectrometry and electrochemical assays and so on are generally utilized for the detection of aluminum ions, but they address main challenges such as high cost instrumentations, lack of selectivity, the requirement of specific operating skills and extensive instrument [13–17]. In this concept, recent decades have witnessed an increasing trend in the application of fluorescent signaling for monitoring of Al (III) ions, since it is a technique with highly sensitive and selective detection and shows functional simplicity, high efficiency, sensitive detection, low cost, non-destructive and so on [18,19].

Fluorescent probes based on the determination of the aluminum ions are emerging as an area of keen interest [20]. Appropriate selection of fluorescent probes allows sensitive and selective determination of aluminum ions in the solutions. In this concept, anthracene, BODIPY, fluorescein, rhodamine, resorufin, coumarin and cyanine based organic molecules have been extensively used as fluorescent probes for the determination of Al^{3+} in solutions [21,22]. Also, thiazolidines have been employed in several research areas since they are associated with

* Corresponding authors.
E-mail addresses: duyguaydin@kmu.edu.tr (D. Aydin), abaran@sakarya.edu.tr (A. Baran).

https://doi.org/10.1016/j.saa.2020.118431
1386-1425/

several biological and antitumor activities, and utilized as antimicrobial, anti-inflammatory and as antiviral agent. Thus, thioazolidones can be used as a promising scaffold to develop drug analogs, or as antimicrobial, anti-inflammatory and antiviral agents [23–25].

Herein, we report the production of two new fluorescent "turn on" probes containing 4-thiazolidine derivative. The probes showed the ultrasensitive and highly selective determination of Al^{3+} in ACN/H_2O (v/v = 50/50, 10 μM, pH = 7.0) solution at 524 nm. Finally, the synthesized fluorescent probes were used as a tool to identify Al^{3+} ions in living cells.

2. Experimental

2.1. General and reagents

In the study, Heidoph Laborota 4001 and Bibby rotary evaporator, were used for removal solvent. Chemicals and solvents (Sigma-Aldrich Co., USA) were purchased commercially suppliers. Thin layer chromatography (TLC on Merck 0.2 mm silica gel 60 F254 analytical aluminum plates) was used for proceeding reaction controls. ^{1}H NMR, ^{13}C NMR and another NMR technique (COSY, HETCOR) were taken on 300 and 600 MHz for ^{1}H NMR and 75 and 150 MHz for ^{13}C NMR spectrometer. IR spectra were realized on Perkin-Elmer 1600 FT-IR instrument (Perkin Elmer, Waltham, MA, USA). Absorption and emission spectra were measured utilizing a Shimadzu (model 2600) UV spectrophotometer and Agilent Technologies Cary Eclipse spectrophotometer, respectively. Elemental (CHNS) and TOF-MS analysis were obtaied via an Perkin-Elmer (Waltham, MA, USA) and Agilent 6230 equipment (Agilent Technologies Inc., Wilmington, DE, USA), respectively.

2.2. Synthesize of the compound 2-(4-hydroxyphenyl)-3-phenylthiazolidin-4-one (1), 2-hydroxy-5-(4-oxo-3-phenylthiazolidin-2-yl)benzaldehyde (1a) and 2,3-bis(4-hydroxy phenyl)thiazolidin-4-one (2)

Compounds **1** and **2** were prepared by slight modification according to reported literature [26,27]. Procedures of compounds **1**, **2**, **1a** and **2a** were given in the supporting information section.

2.3. Synthesis of the probe AM1

2-aminophenol (0.2 g, 1.82 mmol) was added to an absolute ethanol (10 mL) solution of **1a** (0.5 g, 1.67 mmol) and the solution was refluxed for 3 h. After this period, the mixture was cooled down. Obtained precipitate was washed with plenty of water then cold ethanol, dried in vacuo, and then recrystallized from absolute ethanol to obtain orange powder in % 61 yields; Mp 110–112 °C. **^{1}H NMR** (300 MHz, DMSO-d_6): δ(ppm): 8.91 (s, 1H, -CH=N-), 7.64 (d, J = 2.1 Hz, 1H, $H_{4''}$), 7.39–7.24 (m, 6H, H_x, $H_{x'}$, H_y, $H_{y'}$, Hk, $H_{4'}$), 7.28 (m, 2H, $H_{x'''}$, $H_{y'}$), 6.92 (d,1H, J = 8.0 Hz), 6.83 (dd, J = 15.8, 7.3 Hz, 1H, $H_{y'''}$, $H_{x''}$), 6.46 (bs, 1H), 3.94 (q, J = 15.8 Hz, 2H, H_5). **^{13}C NMR** (75 MHz, DMSO-d_6): 196.22, 171.1, 162.0, 161.5, 151.9, 138.3, 135.0, 132.6, 131.7, 130.5, 129.5, 129.0, 127.3, 126.7, 120.3, 120.1, 119.7, 118.0, 117.2, 64.0, 33.5. FT-IR (cm^{-1}): 3620, 3062, 2934, 1623, 1492, 1150, 747, 693. Anal. Calc. for $C_{22}H_{18}N_2O_3S$ (390,46) (%): C, 67.68; H, 4.65; N, 7.17. Found (%): C, 67.72; H, 4.54; N, 7.25.

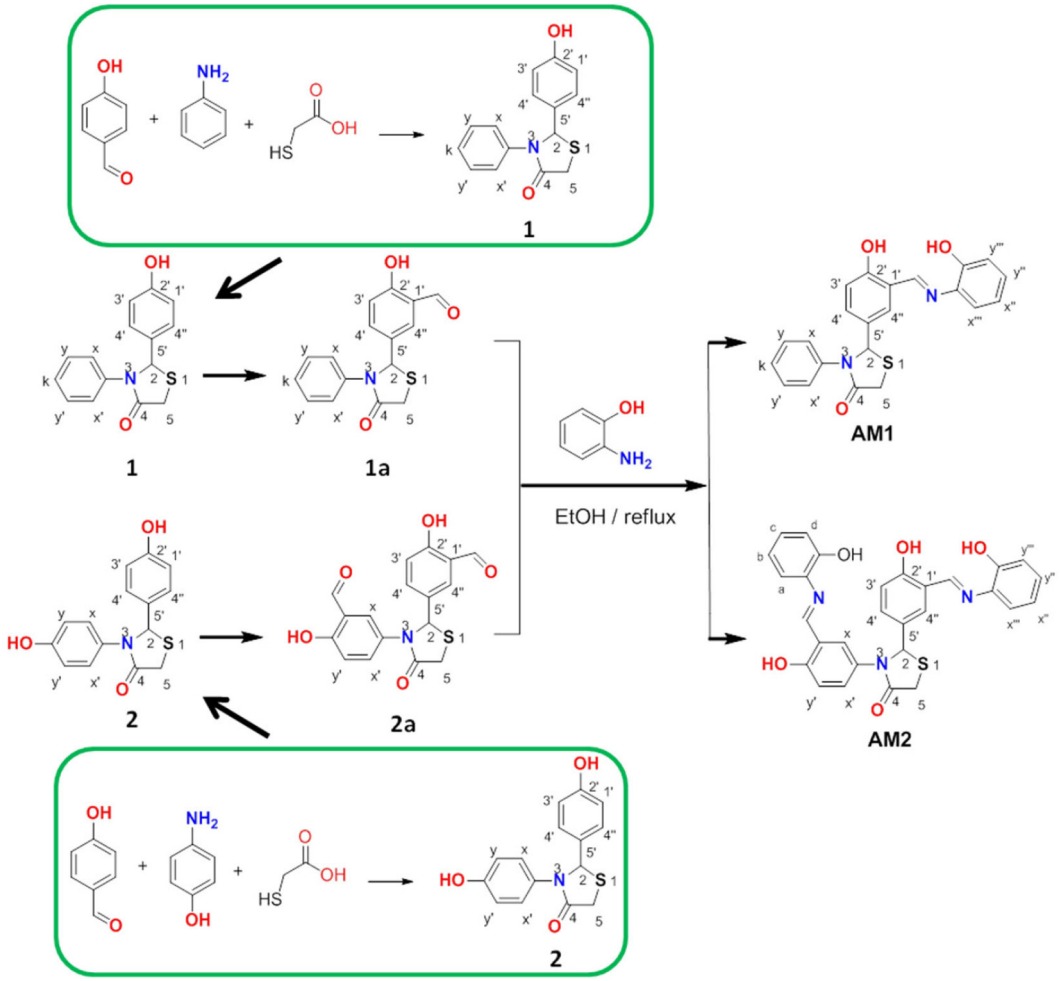

Scheme 1. Synthesis routes of the probe **AM1** and **AM2**.

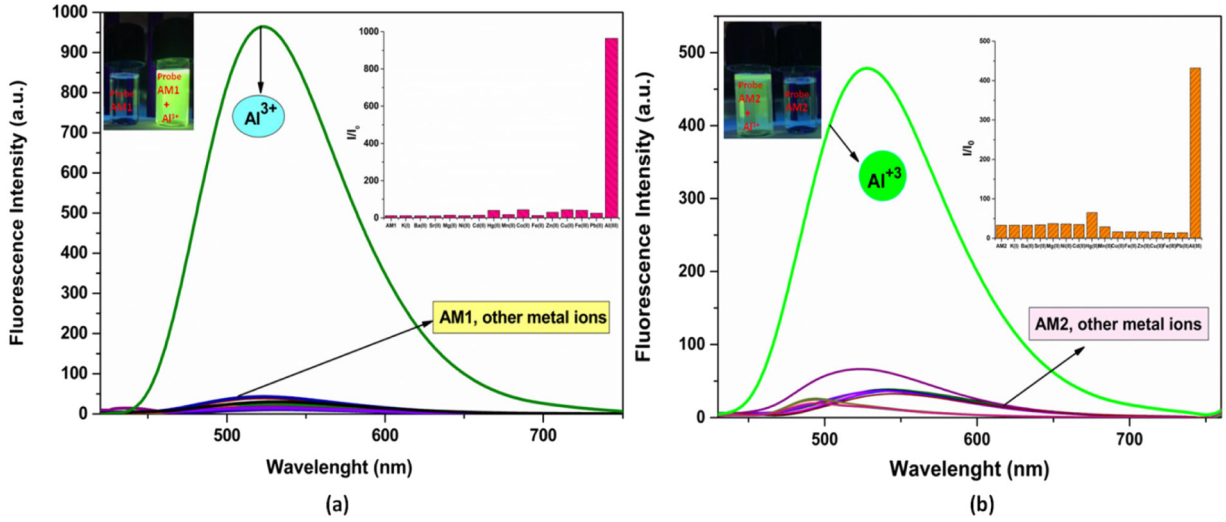

Fig. 1. The fluorescence emission spectra of **AM1** (a) and **AM2** (b) (10 μM in ACN/H_2O (v/v = 50/50) and after addition of 5.0 equiv. of different metal ions (Fe^{2+}, Hg^{2+}, K^+, Co^{2+}, Ni^{2+}, Mg^{2+}, Cd^{2+}, Sr^{2+}, Fe^{3+}, Cu^{2+}, Mn^{2+}, Ca^{2+}, Al^{3+}, Zn^{2+}, Ba^{2+} and Pb^{2+}) (λ_{ex} = 390 nm, slit: 5–10).

2.4. Synthesis of the probe AM2

A solution of 4-oxothiazolidine **2a** (0.2 g, 0,58 mmol) was solved in absolute ethanol (20 mL) and added 2-aminophenol (0.12 g, 1.86 mmol) at rt. and the stirring was maintained in this temperature for a while. Then the temperature was elevated to reflux and left to stand in this temperature for 6 h. Afterwards, the precitated was filtered off, washed with water and recrystallized from cold ethanol to give desired product **AM2** (0.23 g, 75%) as a tile colored solid. mp 110–112 °C. **^{1}H NMR** (600 MHz, DMSO-d_6) δ(ppm): 9.77 (s, 1H, OH), 9.75 (s, 1H, OH), 8.91 (s, 1H, OH), 8.84 (s, 1H, OH), 7.66 (s, 1H, -CH=N), 7.56 (s, 1H, -CH=N), 7.33–7.30 (m, 4H), 7.09 (t, 2H, J = 8.0 Hz), 6.92 (d, 2H, J = 8.0 Hz), 6.83 (d, 4H, J = 8.1 Hz), 6.35 (s, 1H, -CH=, H_2), 4.02 (d, 1H, J = 16.00 Hz, -CH_2-), 3.89 (d, 1H, J = 15.17 Hz, -CH_2-). **^{13}C NMR** (150 MHz, DMSO-d_6) 170.9, 161.7, 161.4, 160.9, 159.8, 151.6, 151.5, 134.92, 134.90, 132.5, 131.6, 130.4, 130.2, 129.0, 128.72, 128.66, 120.04 (3C), 119.91, 119.88, 119.74, 119.51, 117.74, 117.55, 117.0 (2C), 64.0, 33.12. FT-IR (cm^{-1}): 3058, 2943, 2840, 2707, 1663, 1622, 1490, 1356, 1192, 1142, 745. Anal. Calc. for $C_{29}H_{23}N_3O_5S$ (525.58) (%): C, 66.27; H, 4.41; N, 8.00. Found (%): C, 66.17; H, 4.45; N, 7.98.

2.5. Measurement procedures

For fluorescence and UV–Vis measurements, the stock solution of the probe **AM1** and **AM2** was prepared in DMSO (10 mM) and diluted in ACN/H_2O (v/v, 50/50) (10 μM). Perchlorate salts of metals (Fe^{2+}, Hg^{2+}, K^+, Co^{2+}, Ni^{2+}, Mg^{2+}, Cd^{2+}, Sr^{2+}, Fe^{3+}, Cu^{2+}, Mn^{2+}, Al^{3+}, Zn^{2+}, Ba^{2+} and Pb^{2+}) were utilized and solved in deionized water (10 mM). 3 mL probe solution was added to a cuvette to assess the determination of various metal ions. Corresponding volume of perchlorate salts was added into solution of **AM1** and **AM2**. Afterwards, the spectral data of the solution was mesaured by UV–Vis and fluorescence spectroscopy after mixing for 10 min (λ_{ex} = 390 nm, slit widths = 5 nm/10 nm).

2.6. Cell culturing and cytotoxicity testing

Human epithelium Lovo cells were grown in ATCC-formulated F-12K medium supplemented with 10% fetal bovine serum (FBS, Gibco) at 37 °C containing 5% CO_2. To explore the applicibility of sensors in cell imaging, the cytotoxicity of the probe **AM1** and **AM2** on Lovo cells was evaluated. Determination of cell viability and cytotoxicity were performed with Alamar Blue assay as described previously [28]. DMSO was utilized to prepare the stock solutions of **AM1** and **AM2** and then these solutions were diluted with growth medium. The concentration of DMSO was kept under %0.1. Lovo cells were treated with various concentrations of compounds ranging from 1 μM to 200 μM. The IC_{50} values were determined from the reciprocal plot of normalized inhibition (%) compound concentration (Log) by GraphPad Prism 5.0 software. For showing the applicibility of the probes in living cells, the cells were treated with the probe **AM1** and **AM2** (10.0 μM) and incubated for 30 min. To eliminate excess probes, the cells were washed with PBS

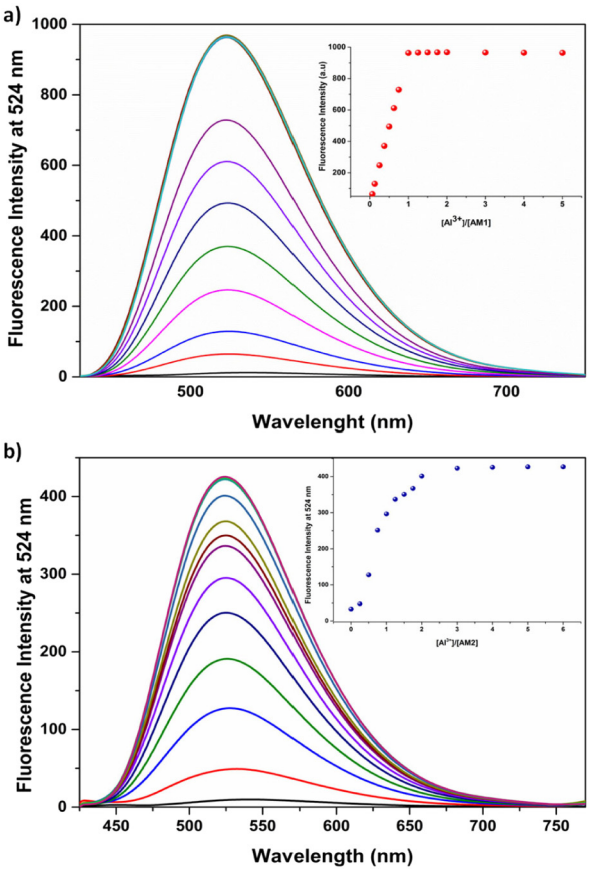

Fig. 2. The fluorescence responds of (a) **AM1** and (b) **AM2** (10 μM) with different concentrations of Al^{3+} (0.0–5.0 equiv) in ACN/H_2O (v/v = 50/50, pH: 7) (λ_{ex} = 390 nm).

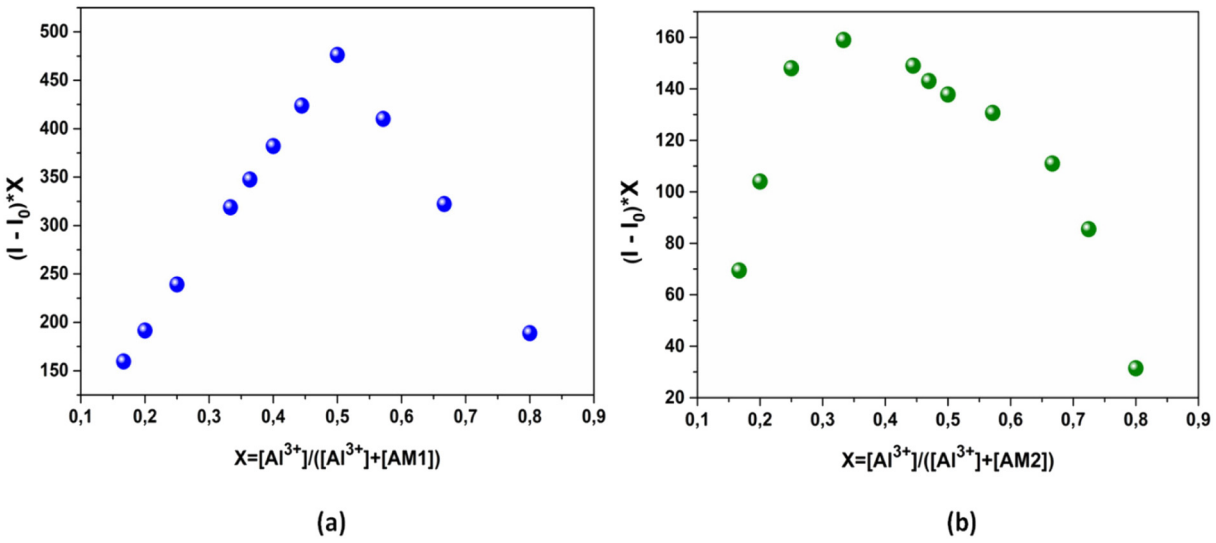

Fig. 3. Job's plots of (a) **AM1**-$Al^{3+}$and (b) **AM2**-Al^{3+} complex in ACN/H_2O (v/v = 50/50, pH 7).

(2 × 10 mM). Afterwards, they were treated with Al^{3+} (100 μM) and reincubated for 30 min. Bio-Rad ZOE fluorescence microscope was used to take images of the cells.

3. Results and discussion

3.1. Fabrication and structural characteristics of the probes AM1 and AM2

The synthetic routes of the probe **AM1** and **AM2** are shown in Scheme 1. The compounds **1**, **2**, **1a**, **2a**, and the probe **AM1** and **AM2**, were synthesized and then the structures of prepared compounds were analyzed by various spectroscopic methods (Figs. S1–S23).

For the characterization of the probe **AM1**, the resonance signals of protons H_2 and H_5 in ^{1}H NMR are shown as in compounds **1** and **2** in supporting information. The H_2 appears as singlet at 6.46 ppm and H_5 appear as quartet at 3.95 ppm. At 8.91 ppm, the azide double band proton signal was resonated as singlet. The other prominent proton belongs to $H_{4''}$ resonated at 7.64 ppm as dublet with coupling constant $J_{4''4'}$ = 2.1 Hz. The H_x, $H_{x'}$, H_y, $H_{y'}$, $_{Hk}$, $H_{4'}$ protons were resonated as multiplet between 7.39 and 7.24 ppm. Other protons $H_{x''}$ and $H_{y'}$ resonate as multiplet at 7.28 ppm. The $H_{3'}$ was resonated at 6.95 ppm as a dublet with coupling constant of $J_{3'4'}$ = 8.0 Hz. The $H_{y''}$ and $H_{x'}$ protons were resonated at 6.83 ppm as dublet of dublet with coupling constant, J = 15.8 and 7.3 Hz respectively (Fig. S9). Twenty-two carbon atoms observed in ^{13}C NMR are compatible with the synthesized structure (Fig. S10). In the IR spectrum, the band belongs to the group -OH at 3262 cm^{-1}. Other striking bands belong to the group -C=O at 1664.13 cm^{-1}, 1623.16 cm^{-1}. The results of the analysis of theoretically calculated elements, C, H, N are in agreement with the experimental results of the same elements.

All hydroxyl group protons from the characterization of the structure of **AM2** were resonated at 9.77 and 9.75 ppm. Then, schiff bases protons were resonated as singlets at 8.91 and 8.84 ppm. Other prominent protons of the molecule are the resonances of H_2 and H_5. The H_2 proton was resonated as singlet at 6.35 ppm and the H_5 proton was resonate as dublet at 4.02 ppm (J = 16.00 Hz) and at 3.89 ppm (J = 15.17 Hz) as dublet respectively (Fig. S22). ^{13}C NMR exhibited a good indication for one carbon of carbonyl group at 170.93 ppm and four hydroxyl bonded carbons at 161.72 ppm, 161.39 ppm, 151.57 ppm, 151.53 ppm. Also, double bond carbons, bounded to nitrogen appear at 160.90 ppm, 159.78 ppm. Other aromatic carbons remaining resonated at 136–115 ppm in the regions they deserve. The other most

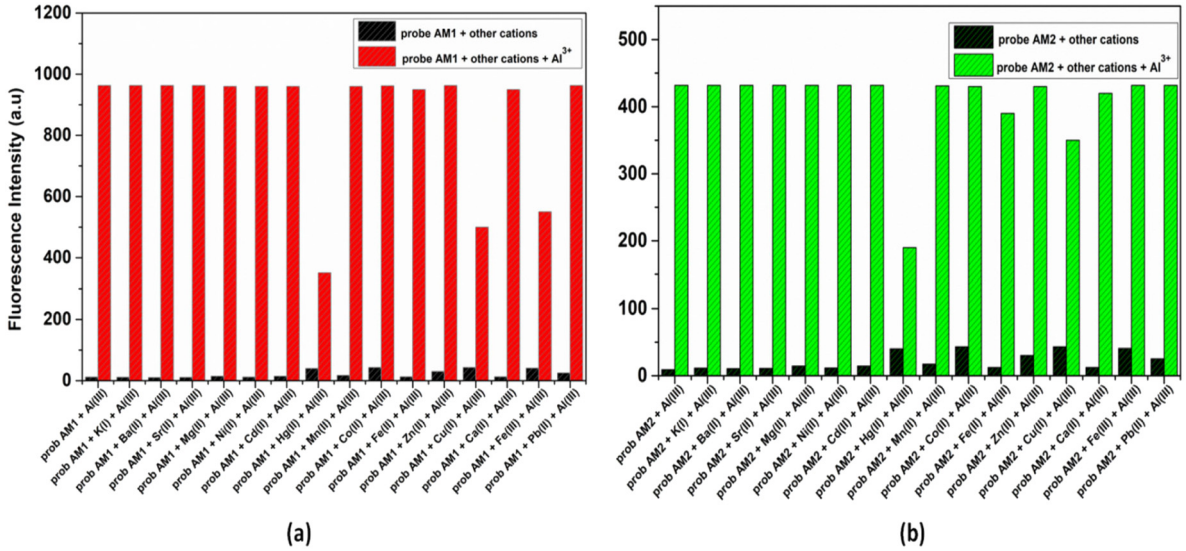

Fig. 4. Interference of other metal ions on the fluorescence intensity of Al^{3+} (5.0 equiv) (a) with **AM1** (10.0 μM) and (b) **AM2** (10.0 μM).

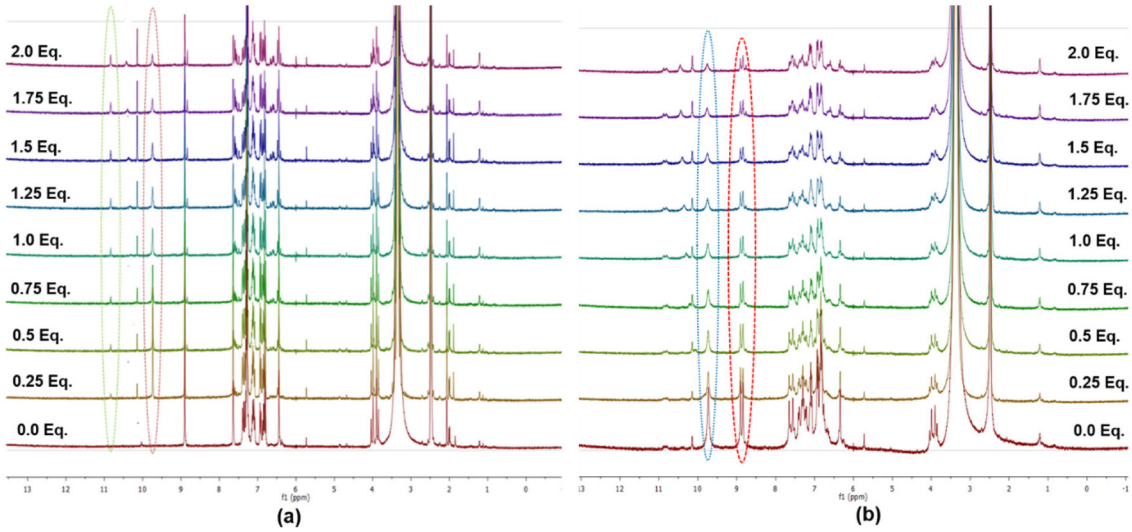

Fig. 5. ^{1}H NMR spectra of (a) **AM1** and (b) **AM2** in presence of various equiv. of Al^{3+}.

striking carbon resonance signals are that appear for the C_2 and C_5 carbons, where C_2 resonance at 64.03 ppm and C_5 at 33.12 ppm (Fig. S23). In the analysis of FT-IR spectrum for probe **AM2**, the -OH group bands appeared at 3058 and 2943 cm^{-1}. The carbonyl group bands appeared at 1663.93 cm^{-1} and 1621.67 cm^{-1}. These NMR results are consistent with the structure and the element analysis results correspond to the structure.

3.2. Fluorogenic sensing for Al^{3+} in ACN/H_2O

Solutions of the both of the chemosensor **AM1** and **AM2** in ACN/H_2O (v/v = 50/50, 10 μM, pH = 7.0) solution were colorless at 524 nm and gave negligible fluorescence emission after excitation at 390 nm due to the PET (Photo-induced electron transfer) and C=N isomerisation mechanisms from the imine nitrogen to the thiazolidine unit. However, after the adding of various metal ions (Zn^{2+}, K^{+}, Hg^{2+}, Al^{3+}, Co^{2+}, Mg^{2+}, Sr^{2+}, Ni^{2+}, Cd^{2+}, Ba^{2+}, Mn^{2+}, Fe^{2+}, Cu^{2+}, Ca^{2+}, Fe^{3+} and Pb^{2+}) (5.0 equiv.) to **AM1** and **AM2** in ACN/H_2O (v/v = 50/50, 10 μM, pH = 7.0) solution, each sensing compound exhibited remarkable selective and sensitive response to Al^{3+} ions in same apparent colors while other metal cations cause almost no fluorescence increase (Fig. 1).

The -C=N- groups in the probe **AM1** and **AM2** act as electrondonors and the formation of the stable chelation between each probe and Al^{3+} might be suppressed by the PET and C=N isomerisation process in the probes and so lead strong fluorescence enhancement (Scheme 1). The complex between **AM1** and Al^{3+} has strong green emission with the maximum emission wavelength (λ_{em} = 524 nm, λ_{ex} = 390 nm), and also the **AM2**-Al^{3+} showed an obvious "turn-on" response toward Al^{3+} at λ_{em} = 524 nm. As a result of the additional thiazolidine and amine substituents, the HOMO-LUMO band gaps of **AM2** reduced and also radiactive decay process was affected. These results suggested that the complex formation between each probe (**AM1** and **AM2**) and Al^{3+} was accomplished and strong fluorescence turn on behavior at 524 nm against aluminum ions could be easily observed.

In order to assess the sensitivity of the fabricated probe **AM1** and **AM2** against Al^{3+}, the fluorescence intensity of the probe **AM1** and **AM2** solutions were recorded in 2 min following in the presence of Al^{3+} ions and the results were demonstrated in Fig. 2a and b. As a result of the gradual addition of Al^{3+} (0.0–5.0 equiv) to the **AM1** and **AM2** solutions (10.0 μM), the emission intensity for **AM1** and **AM2** at 524 nm increased and remained constant after the adding of 1.0 and 2.0 equiv. of Al^{3+} concentration for **AM1** and **AM2**, respectively (Fig. 2a and b).

The Job plots demonstrated Al^{3+}/AM1 and Al^{3+}/AM2 to have 1:1 and 2:1 metal/ligand ratio, respectively (Fig. 3a and b). The association constants (K_a) as determined by fluorescence titration method for each sensors with Al^{3+} were calculated to be 7.7 × 10^3 M^{-1} for Al^{3+}/AM1 and 3.1 × 10^{10} M^{-2} for Al^{3+}/AM2 (Fig. S25a and b) [29].

To assign LOD of the probe **AM1** and **AM2**, linear the emission intensity plots for **AM1** and **AM2** with the Al^{3+} concentration in nanomolar levels were determined. LOD values (LOD = 3 std./K) [30,31] of the probe **AM1** and **AM2** are 0.11 μM and 4.4 μM, respectively and these values are below the permitted limit values of 7.41 μM for aluminum (III) ions in the World Water Organization's drinking water guidelines (Fig. S26a and b) [4].

Furthermore, the UV–visible absorption bands of each sensor were investigated in ACN/H_2O (v/v = 50/50, 10 μM, pH = 7.0) solution. The absorption bands of **AM1** and **AM2** (10.0 μM) were observed at 320 nm and 440 nm for **AM1** and **AM2** and it could easily said that these bands associated with n–π* and π–π* transitions in sensors. After the addition of the Al^{3+} ions (5.0 equiv.), the absorption bands of **AM1** and **AM2** demonstrated the large spectral bathochromic shifted showing deprotonation of the hydroxyl of the phenol unit to allow the probes binding with Al^{3+}. Upon cation recognition process, the λ_{max} of **AM1** at 320 and 440 nm reduced and a novel band at 420 nm was observed because the band at 440 bathochromically shifted. Also, the λ_{max} of **AM2** shifted from 440 nm and 420 nm (Fig. S27a and b).

As a next step, the selectivity study of **AM1** and **AM2** toward Al^{3+} in the presence of different metal ions was performed. The fluorescence spectroscopy was utilized for selectivity studies and enabled us to

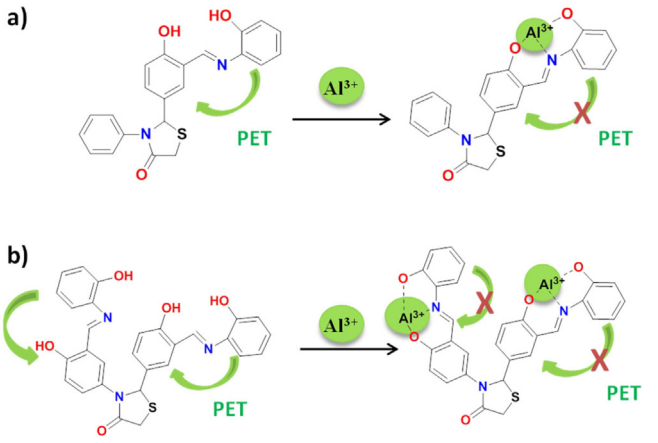

Scheme 2. Proposed sensing mechanisms and binding modes of (a) **AM1** and (b) **AM2** with aluminum (III) ions.

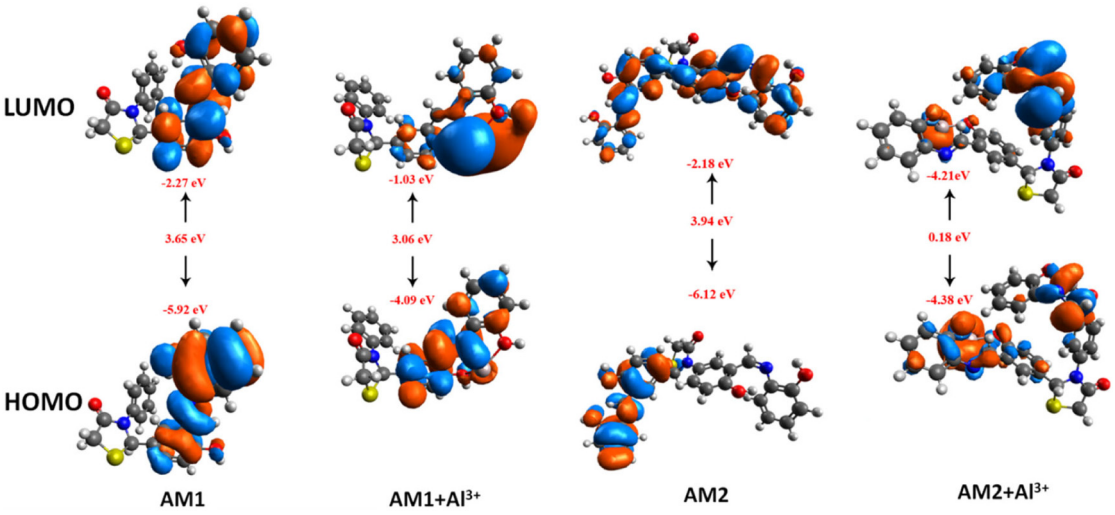

Fig. 6. The optimized configurations along with the HOMO and LUMO distributions of the probe AM1 and AM2 and the AM1-Al^{3+} and AM2-Al^{3+} complexes.

understand the possible interference from other competitive metal ions in determination of Al^{3+}. As shown in Fig. 4a and b, the other metal ions induced either a negligible change or some quenching in the fluorescence intensity of probe **AM1**-Al^{3+} and **AM2**-Al^{3+}, only addition of Hg^{2+} and Cu^{2+} and Fe^{3+} induced a slightly decrease of fluorescence. These results clearly displayed that the fabricated probes, **AM1** and **AM2**, have selectivity for the sensing of Al^{3+} ions in the presence of even competing various cations.

In addition, pH range plays critical roles in sensors, so generally sensors must function over a suitable physiological pH range to be usable for their biological applications. The best results for the sensitivity of **AM1**-Al^{3+} and **AM2**-Al^{3+} were obtained at pH = 7. The probe **AM1** and **AM2** displayed a remarkable turn on fluorescence signal at pH = 7 after adding of Al^{3+} ions. However, fluorescence intensities of **AM1**-Al^{3+} and **AM2**-Al^{3+} decreased due to the competition of -OH ions interacted with Al^{3+}coordination at high pH values (Fig. S28).

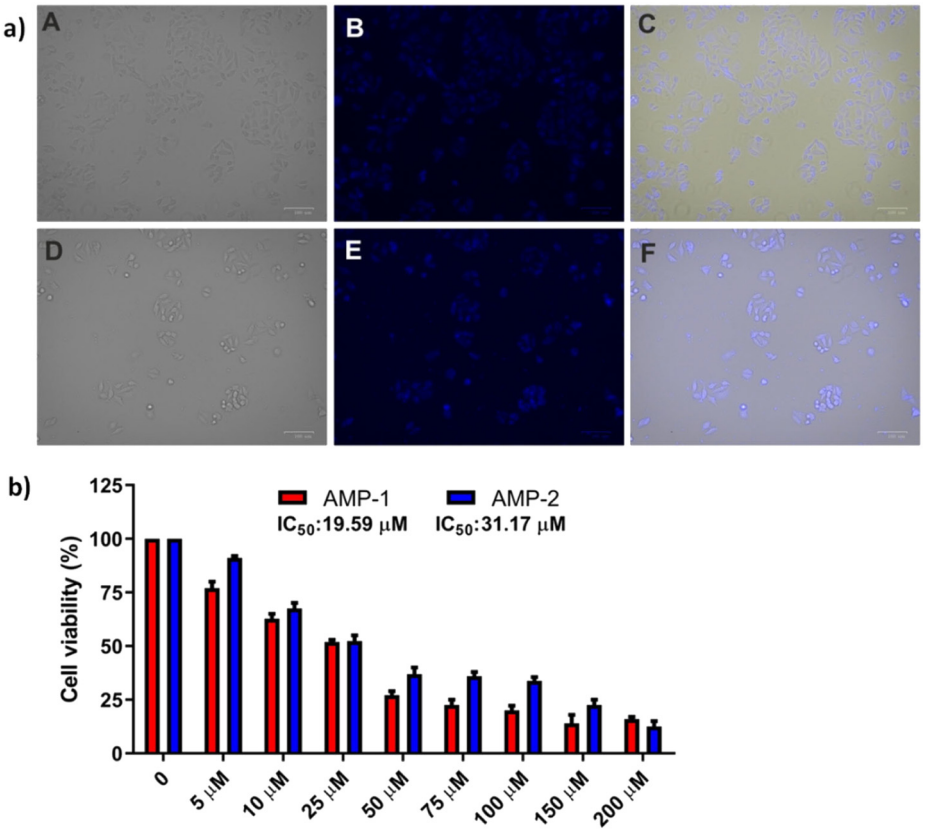

Fig. 7. (a) Fluorescence images of Human epithelium Lovo cells: A for **AM1** and D for **AM2** represent bright field images of the cells treated with the probes (10.0 μM) for 30 min. Images (B for AM1 and E for AM2) represent the fluorescence images of A for AM1 and D for AM2 in the presence of Al (III) ions for 30 min. C for AM1 and F for AM2 represent the merged images of the bright-light field (A) and (D), and also fluorescence (B) and (E). (b) Cytotoxicity graphs of the probes AM1 and AM2. Scale bar = 100 μm, $\lambda_{Blue\text{-}channel\text{-}ex}$: 355/40 nm; $\lambda_{Blue\text{-}channel\text{-}em}$: 433/36 nm.

3.3. The proposed interaction mechanism for AM1-Al^{3+} and AM2-Al^{3+}

^{1}H NMR titration was carried out to deeper understand the binding mode of probe **AM1**- and **AM2** with Al^{3+}. In free **AM1**, imine proton signal in DMSO-d_6 was appeared at 8.91 ppm. Upon interaction with 1.0 equiv. of Al^{3+}, two novel signals formed at 10.9 ppm and 9.8 ppm which clearly indicated the deprotonation of hydroxyl proton by interaction with Al^{3+}(Fig. 5a). In the probe **AM2**, hydroxyl protons of the phenol units at 9.77 and 9.75 ppm, and also imine proton signals at 8.91 and 8.84 ppm were appeared. Both hydroxyl protons of the phenol at 9.77 and 9.75 ppm and imine proton signals at 8.91 and 8.84 ppm gradually decreased as a result of the increasing concentration of Al^{+3}, indicating the complex formation between the oxygen, nitrogen atom and Al^{3+} (Fig. 5a and b).

Based on the above results from ^{1}H NMR titration and job's plot, the possible complex structure of **AM1**-Al^{3+} and **AM2**-Al^{3+} has been shown in Scheme 2.

Additionally, density functional theory (DFT) was used to verify the optimized configurations and HOMO and LUMO energy levels of the probe **AM1** and **AM2** and the **AM1**-Al^{3+} and **AM2**-Al^{3+} complexes. B3LYP and 3-21G/Lanl2dz basis set parametes were utilized to optimize Gaussian 09 software. As shown in Fig. 6, it is clear that the HOMO and LUMO are distributed different parts of **AM1** and **AM2** and the **AM1**-Al^{3+} and **AM2**-Al^{3+}. The energy gap between HOMO and LUMO orbitals of **AM1** and **AM2** are 3.65 and 3.94, respectively while these gaps are 3.06 and 0.18 eV for the **AM1**-Al^{3+} and **AM2**-Al^{3+}. From these calculation, it is easily said that the probe **AM1** and **AM2** form stable **AM1**-Al^{3+} and **AM2**-Al^{3+} complexes as evident from the lower HOMO–LUMO energy gaps of the complexes compared to the probe **AM1** and **AM2** (Fig. 6).

3.4. Bio-imaging applications

As a model application, the Human epithelium Lovo cells were utilized for fluorescence imaging of the **AM1** and **AM2** against Al^{3+} in the live cells. Human epithelium Lovo cells were grown in ATCC-formulated F-12K medium. The cells were incubated with **AM1** and **AM2** and no fluorescence were obtained. After the addition of Al^{3+} ions to the **AM1** and **AM2** pretreated cell medium, it was found that each sensor in the cell medium could achieve the Al^{3+} detection behavior as in the solution medium (Fig. 7a). Moreover, the cell viability assays show that the probe **AM1** and **AM2** are partially toxic (Fig. 7b). Suprisingly, it was evident that cells threated with **AM2** led to lower cell death than cells threated with **AM1** (Fig. 7b). Overall, developing **AM1** and **AM2** sensors could be utilized as probes to detect Al^{3+} in living cells.

4. Conclusion

In summary, two novel thiazole–based fluorescent sensors (**AM1** and **AM2**) were designed and fabricated and the sensors offer realistic potential for the trace monitoring of Al^{3+} in the presence of various metal cations in ACN/H_2O (v/v = 50/50, 10.0 μM, pH = 7.0). Prepared probes **AM1** and **AM2** are capable of the determination of Al^{3+} via turn on fluorescence emission because of the prevention of PET. The limits of detection were calculated as 0.11 μM for **AM1** and 4.40 μM for **AM2** on the basis of $3\sigma/k$ and these values were below WHO guideline for drinking water. The binding mode of **AM1**/$\mathbf{Al^{3+}}$ and **AM2**/$\mathbf{Al^{3+}}$ was established by the Job method and found to be 1:1 and 1:2 ratio, respectively. Also, both in vitro cytotoxicity and fluorescence microscopy images in living cells point out the ability of these sensors for sensing of Al^{3+}. Overall, the thiazolidine based chemosensors for determining of aluminum ions outlined here provides an attractive and tunable platform for fluorescent detection of Al^{3+} in biological applications.

CRediT authorship contribution statement

Duygu Aydin: Supervision, Investigation, Methodology, Conceptualization, Formal analysis, Writing - original draft.**Emel Karakilic:**Investigation.**Serdar Karakurt:**Investigation.**Arif Baran:**Supervision, Methodology, Conceptualization, Formal analysis.

Declaration of competing interest

The authors declare that they have no known competing financial interests or personal relationships that could have appeared to influence the work reported in this paper.

Acknowledgements

The authors are indebted to the TÜBITAK (Scientific and Technological Research Council of Turkey with grant number 217Z043) and the KMU Scientific Research Project Center for their support with the project 30-M-16 to provide the Gaussian 09W and Gauss view 5.0.8 programs. Also, authors thank Abdurrahman KARAGOZ for help with DFT studies.

Appendix A. Supplementary data

Supplementary data to this article can be found online at https://doi.org/10.1016/j.saa.2020.118431.

References

[1] D. Maity, T. Govindaraju, Conformationally constrained (Coumarin-Triazolyl-Bipyridyl) click fluoroionophore as a selective Al^{3+} sensor, Inorg. Chem. 49 (2010) 7229–7231, https://doi.org/10.1021/ic1009994.
[2] Y. Lu, S. Huang, Y. Liu, S. He, L. Zhao, X. Zeng, Highly selective and sensitive fluorescent turn-on chemosensor for Al^{3+} based on a novel photoinduced electron transfer approach, Org. Lett. 13 (2011) 5274–5277, https://doi.org/10.1021/ol202054v.
[3] W.H. Ding, W. Cao, X.J. Zheng, D.C. Fang, W.T. Wong, L.P. Jin, A highly selective fluorescent chemosensor for Al(III) ion and fluorescent species formed in the solution, Inorg. Chem. 52 (2013) 7320–7322, https://doi.org/10.1021/ic401028u.
[4] Z. Li, C. Liu, J. Wang, S. Wang, L. Xiao, X. Jing, Spectrochimica Acta Part A: molecular and biomolecular spectroscopy A selective diaminomaleonitrile-based dual channel emissive probe for Al^{3+} and its application in living cell imaging, Spectrochim. Acta A Mol. Biomol. Spectrosc. 212 (2019) 349–355, https://doi.org/10.1016/j.saa.2019.01.031.
[5] J. Fu, K. Yao, Y. Chang, B. Li, L. Yang, K. Xu, Spectrochimica Acta Part A: Molecular and Biomolecular Spectroscopy A novel colorimetric-fluorescent probe for Al^{3+} and the resultant complex for F^- and its applications in cell imaging, Spectrochim. Acta A Mol. Biomol. Spectrosc. 222 (2019), 117234. https://doi.org/10.1016/j.saa.2019.117234.
[6] J. Fu, B. Li, H. Mei, Y. Chang, K. Xu, Spectrochimica Acta Part A: Molecular and Biomolecular Spectroscopy Fluorescent schiff base probes for sequential detection of Al^{3+} and F^- and cell imaging applications, Spectrochim. Acta A Mol. Biomol. Spectrosc. 227 (2020), 117678. https://doi.org/10.1016/j.saa.2019.117678.
[7] Q. Huang, T. Wang, N. Xiao, Spectrochimica Acta Part A: Molecular and Biomolecular Spectroscopy Selective monitoring ATP using a fluorogenic Al(III) probe complex in aqueous medium, Spectrochim. Acta A Mol. Biomol. Spectrosc. 229 (2020) 117946, https://doi.org/10.1016/j.saa.2019.117946.
[8] J. Tian, X. Yan, H. Yang, F. Tian, A novel turn-on Schiff-base fluorescent sensor for aluminum(III) ions in living cells, RSC Adv. 5 (2015) 107012–107019, https://doi.org/10.1039/c5ra17557g.
[9] K. Boonkitpatarakul, J. Wang, N. Niamnont, B. Liu, L. Mcdonald, Y. Pang, M. Sukwattanasinitt, Novel turn-on fluorescent sensors with mega stokes shifts for dual detection of Al^{3+} and Zn^{2+}, ACS Sensors 1 (2016) 144–150, https://doi.org/10.1021/acssensors.5b00136.
[10] B. Liu, P.F. Wang, J. Chai, X.Q. Hu, T. Gao, J. Bin Chao, T.G. Chen, B.S. Yang, Naphthol-based fluorescent sensors for aluminium ion and application to bioimaging, Spectrochimica Acta - Part A: Molecular and Biomolecular Spectroscopy 168 (2016) 98–103, https://doi.org/10.1016/j.saa.2016.06.002.
[11] L.Q. Yan, Y. Ma, M.F. Cui, Z.J. Qi, A novel coumarin-based fluorescence chemosensor containing l-histidine for aluminium(III) ions in aqueous solution, Anal. Methods 7 (2015) 6133–6138, https://doi.org/10.1039/c5ay01466b.
[12] X. Sun, Y.W. Wang, Y. Peng, A selective and ratiometric bifunctional fluorescent probe for Al^{3+} ion and proton, Org. Lett. 14 (2012) 3420–3423, https://doi.org/10.1021/ol301390g.
[13] X. Leng, W. Xu, C. Qiao, X. Jia, Y. Long, B. Yang, New rhodamine B-based chromofluorogenic probes for highly selective detection of aluminium(III) ions and their application in living cell imaging, RSC Adv. 9 (2019) 6027–6034, https://doi.org/10.1039/c8ra09850f.

[14] O. Alici, S. Erdemir, A cyanobiphenyl containing fluorescence “turn on” sensor for Al^{3+} ion in CH_3CN–water, Sensors Actuators B Chem. 208 (2015) 159–163, https://doi.org/10.1016/j.snb.2014.11.033.
[15] S. Erdemir, M. Yuksekogul, S. Karakurt, O. Kocyigit, Dual-channel fluorescent probe based on bisphenol A-rhodamine for Zn^{2+} and Hg^{2+} through different signaling mechanisms and its bioimaging studies, Sensors Actuators B Chem. 241 (2017) 230–238, https://doi.org/10.1016/j.snb.2016.10.082.
[16] A. Sahana, A. Banerjee, S. Das, S. Lohar, D. Karak, B. Sarkar, S. Kanti Mukhopadhyay, A.K. Mukherjee, D. Das, A naphthalene-based Al^{3+} selective fluorescent sensor for living cell imaging, Org. Biomol. Chem. 9 (2011) 5523–5529, https://doi.org/10.1039/c1ob05479a.
[17] S. Erdemir, Fluorometric dual sensing of Hg^{2+} and Al^{3+} by novel triphenylamine appended rhodamine derivative in aqueous media, Sensors Actuators B Chem. 290 (2019) 558–564, https://doi.org/10.1016/j.snb.2019.04.037.
[18] S. Kim, J.Y. Noh, K.Y. Kim, J.H. Kim, H.K. Kang, S.W. Nam, S.H. Kim, S. Park, C. Kim, J. Kim, Salicylimine-based fluorescent chemosensor for aluminum ions and application to bioimaging, Inorg. Chem. 51 (2012) 3597–3602, https://doi.org/10.1021/ic2024583.
[19] D. Aydin, A novel turn on fluorescent probe for the determination of Al^{3+} and Zn^{2+} ions and its cells applications, Talanta 210 (2020), 120615. https://doi.org/10.1016/j.talanta.2019.120615.
[20] L. Bai, Y. Xu, G. Li, S. Tian, L. Li, F. Tao, A. Deng, S. Wang, L. Wang, A highly selective turn-on and reversible fluorescent chemosensor for Al^{3+} detection based on novel salicylidene schiff base-terminated PEG in pure aqueous solution, Polymers 11 (2019)https://doi.org/10.3390/polym11040573.
[21] M.K. Alici, Phentroimidazole based fluorescence “turn on” sensor for highly sensitive detection of Zn^{2+} ions, J. Fluoresc. 30 (2020) 269–273, https://doi.org/10.1007/s10895-020-02498-y.
[22] A. Gupta, N. Kumar, A review of mechanisms for fluorescent “turn-on” probes to detect Al^{3+} ions, RSC Adv. 6 (2016) 106413–106434, https://doi.org/10.1039/c6ra23682k.
[23] A.K. Jain, A. Vaidya, V. Ravichandran, S.K. Kashaw, R.K. Agrawal, Recent developments and biological activities of thiazolidinone derivatives: a review, Bioorganic and Medicinal Chemistry 20 (2012) 3378–3395, https://doi.org/10.1016/j.bmc.2012.03.069.
[24] A.C. Tripathi, S.J. Gupta, G.N. Fatima, P.K. Sonar, A. Verma, S.K. Saraf, 4-Thiazolidinones: the advances continue, Eur. J. Med. Chem. 72 (2014) 52–77, https://doi.org/10.1016/j.ejmech.2013.11.017.
[25] H.M. Hosni, M.M. Abdulla, Anti-inflammatory and analgesic activities of some newly synthesized pyridinedicarbonitrile and benzopyranopyridine derivatives, Acta Pharma. 58 (2008) 175–186, https://doi.org/10.2478/v10007-008-0005-4.
[26] R.R. Harale, P.V. Shitre, B.R. Sathe, M.S. Shingare, Pd nanoparticles: an efficient catalyst for the solvent-free synthesis of 2,3-disubstituted-4-thiazolidinones, Res. Chem. Intermed. 42 (2016) 6695–6703, https://doi.org/10.1007/s11164-016-2490-2.
[27] M. Sala, A. Chimento, C. Saturnino, I.M. Gomez-Monterrey, S. Musella, A. Bertamino, C. Milite, M.S. Sinicropi, A. Caruso, R. Sirianni, P. Tortorella, E. Novellino, P. Campiglia, V. Pezzi, Synthesis and cytotoxic activity evaluation of 2,3-thiazolidin-4-one derivatives on human breast cancer cell lines, Bioorganic and Medicinal Chemistry Letters 23 (2013) 4990–4995, https://doi.org/10.1016/j.bmcl.2013.06.051.
[28] S. Karakurt, Modulatory effects of rutin on the expression of cytochrome P450s and antioxidant enzymes in human hepatoma cells, Acta Pharma. 66 (2016) 491–502, https://doi.org/10.1515/acph-2016-0046.
[29] K. Aich, S. Goswami, S. Das, C. Das Mukhopadhyay, A new ICT and CHEF based visible light excitable fluorescent probe easily detects in vivo Zn^{2+}, RSC Adv. 5 (2015) 31189–31194, https://doi.org/10.1039/c5ra03353e.
[30] S. Nihan, K. Elmas, Z. Emine, A. Serol, A. Bostanci, I. Yilmaz, A novel fl uorescent probe based on isocoumarin for Hg^{2+} and Fe^{3+} ions and its application in live-cell imaging, Spectrochimica Acta Part A: Molecular and Biomolecular Spectroscopy 224 (2020) 3–10, https://doi.org/10.1016/j.saa.2019.117402.
[31] S. Nihan, K. Elmas, I.B. Gunay, K. Koran, D. Aydin, F.N. Arslan, A.O. Gorgulu, An ultrasensitive and selective ‘turn off’ fluorescent sensor with simple operation for the determination of trace copper(II) ions in water and various beverage samples, Supramol. Chem. 31 (2019) 756–766, https://doi.org/10.1080/10610278.2019.1702195.